JOURNAL OF MATERIALS SCIENCE **37** (2002) 3981 – 3986

Electrode characteristics of $Li_2Ti_3O_7$-ramsdellite processed by mechanical grinding

M. E. ARROYO Y DE DOMPABLO
Departamento de Química Inorgánica, Fac. Químicas, Universidad Complutense de Madrid, 28040 Madrid, Spain

J. GARCÍA, A. VÁREZ
Departamento de Materiales, Universidad Carlos III de Madrid, Avda. Universidad 30, 28911 Leganés, Spain

F. GARCÍA-ALVARADO
Departamento de Química Inorgánica y Materiales, Facultad de Ciencias Experimentales y Técnicas, Universidad San Pablo CEU, Urbanización Montepríncipe, 28668 Madrid, spain

The effect of mechanical grinding on the electrochemical properties of $Li_2Ti_3O_7$ regarding lithium insertion is studied. X-ray diffraction experiments of milling compounds showed a progressively amorphization of the crystalline material due to both crystalline size decreasing and internal strain increasing. These structural modifications are reflected in the electrochemical behavior of $Li_2Ti_3O_7$, when it is used as the positive electrode in lithium cells. As a function of milling time a higher specific capacity is obtained during the first discharge of the cell, but when charging an increasing in the irreversible capacity is observed. The most promising $Li_2Ti_3O_7$ based electrode has been achieved, under our experimental conditions, for 13 hours milling that produces a compound with crystallite size of approximately 20 nm.

1. Introduction

Insertion compounds are presently being used as electrodes in some battery systems. In these compounds, metallic ions can be reversibly inserted into and extracted from a host structure. The inserted cations are located into a vacant network while the corresponding electrons are donated to the available electronic states of the host. Among the oxides pointed out as candidates to lithium insertion electrode, the compound $Li_2Ti_3O_7$ was recently proposed by M.E. Arroyo y de Dompablo *et al*. [1]. It adopts a ramsdellite type-structure, which framework presents both vacancies in the tunnel of the structure and Ti^{4+} ions capable of being reduced. These facts allow lithium insertion in a reversible mode [2, 3] being the maximum lithium inserted of 2.24 ions per formula [1]. Furthermore, this material presents good cyclability and low polarization, which besides to both the relatively high specific capacity (235 Ah kg^{-1}) and the low average insertion voltage (1.5 V), make this compound a promising material as negative electrode for rechargeable lithium ion batteries.

It is well known that for most type of materials Mechanical Grinding (MG) leads to materials in fine particle form. This process could result in the modification of the quantity of lithium involved in insertion and de-insertion reactions. In this sense, MG has been successfully used for producing amorphous materials (typically alloys) which absorb and release electrochemically large amounts of hydrogen at room temperature [4–8]. In the field of lithium batteries, previous studies have shown that mechanical grinding improves the electrochemical performance of some electrode materials [9, 10]. Regarding the possible application of $Li_2Ti_3O_7$ as anode material, we have analyzed the electrode characteristics of $Li_2Ti_3O_7$ processed by mechanical grinding. We already know that the reversibility of the insertion process in this ramsdellite is good, but in comparison with other anode materials the capacity is lower. The aim of this study was the improvement of the specific capacity of the mentioned material and therefore we have investigated the influence of MG in the specific capacity of cells cycled out of the equilibrium conditions.

2. Experimental

The active material, $Li_2Ti_3O_7$, was prepared by solid state reaction of the stoichiometric amount of Li_2CO_3 and TiO_2 as previously described [1]. Mechanical grinding (MG) was carried out in a centrifugal ball mill (Fritsch, Pulverisette n° 7). This mill generates a high shear interaction as the result of the ball rolling on the wall of the grinding vial [11]. Two sets of experiments were performed using a container (250 cm^3) and grinding balls made from either agate or austenite stainless steel (ASS). In all the experiments the balls-to-powder ratio was 10 : 1 with a powder mass of 25 and 7 g for agate and ASS vial respectively. The rotation speed of

the plate was 500 r.p.m. and the turn way was inverted every 5 minutes approximately.

Structural changes of the MG powder were analyzed by X-ray Diffraction (XRD) using a Philips X'Pert powder automatic diffractometer with Cu Kα radiation ($\lambda = 1.5418$ Å) operating at 40 kV and 50 mA. For the starting material data were recorded between $2\theta = 10$ and 70° with 0.02° step size and 10 s counting time. From these data, unit cell parameters were obtained by a full pattern matching refinement using FULLPROF Program [12]. In the case of milled materials the counting time was reduced to 2 s. For every peak, defined by it Bragg angle, the width (β_{exp}) was measured as the full width at half maximum (FWHM) and the instrumental broadening (β_{inst}) was removed according to

$$\beta^2_{sample} = \beta^2_{exp} - \beta^2_{inst}$$

where β_{sample} is the broadening due to the sample itself. Instrumental broadening was determined from a polycrystalline NIST silicon standard.

As a first step, the evolution of the crystallite size (in Å) was calculated from the Scherrer formula

$$L = K\lambda/\beta_{sample} \cos\,\theta$$

where L is the coherent scattering length ("crystalline size"), K is a constant depending on both the apparatus and the studied sample ($0.9 < K < 1$), λ is the X-Ray wavelength (in Å), β_{sample} is the integral width of the sample (in radians) and θ is the diffraction angle. In a second step, and due to that in some cases the Scherrer equation may under-evaluates the crystallite size, we have used the Hall-Williamson formula [13],

$$\beta_{sample} \cos\,\theta = K\lambda/L + 2\,\varepsilon \sin\,\theta$$

Finally, X ray data were also analyzed using Maud Program [14] that it is a multiple line profile software.

The morphology and the contamination of the samples were evaluated by means of Philips XL-30 scanning electron microscope operating at 20 kV and doted with an Energy Dispersive Spectroscopy detector (EDAX DX4i). All the EDS analyses were registered at the same conditions of voltage (20 kV), working distance, take-off angle and live time (60 sec.).

Electrochemical lithium insertion was carried out using Swagelok-type cells [15] bearing metallic lithium as the negative electrode. For the positive electrode a mixture of the corresponding milled $Li_2Ti_3O_7$, carbon black, and a copolymer of vinyldiene fluoride with hexafluoropropylene (PVDF-HFP) in an 85 : 10 : 5 weight ratio was conformed in a 5 mm-diameter pellet. A 1 M solution of $LiPF_6$ in a mixture of ethylene carbonate (EC) and dimethylcarbonate (DMC), 1 : 1 by volume was used as the electrolyte. After assembling the cells in an argon filled glove box, they were connected to a multichannel galvanostatic-potentiostatic system of the MacPile type [16]. In the galvanostatic mode cell were run under a constant current density of 0.25 mA/cm^2 and at a rate of c/40 (1 Li in 40 hours). From both the elapsed time and the amount of current, the quantity of intercalated lithium, x, in $Li_2Ti_3O_7$ was deduced. In some other cases, cells were discharged under potentiostatic step conditions with a scan rate of 20 mV/h.

3. Results and discussion

3.1. Characterization of MG $Li_2Ti_3O_7$

The X-ray diffraction pattern of the $Li_2Ti_3O_7$ starting material is shown in Fig. 1. All diffraction peaks are indexed according to an orthorhombic (S.G. = Pbnm) unit cell with parameters $a = 5.0164(4)$ Å, $b = 9.54202(8)$ Å and $c = 2.9469(2)$ Å, which are close to previously reported values [1, 17]. In Fig. 2, XRD patterns of the powders, after various milling times into the agate container, are presented together with that of the fresh material ($t = 0$). It can be observed that the milling process makes that both Bragg peaks become much broader and their intensities decrease, in particular those at high diffraction angles. This phenomenon is most noticeable during the first 20 hours. After 32 hours of milling a diffuse halo typical of amorphous materials is observed close to the most intense peak. Another important aspect, is the absence of extra peaks for long milling times, indicating that at least, this material is stable since it does not decompose into other crystalline oxides, as it occurs in other systems [18, 19].

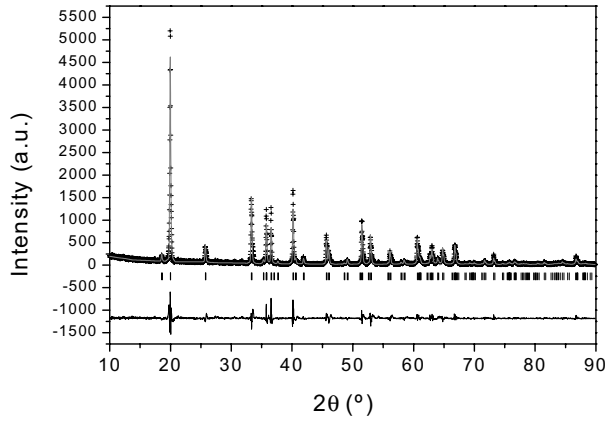

Figure 1 X-Ray diffraction patterns of the starting $Li_2Ti_3O_7$ powders. The crosses correspond to the observed data, and the continous line the least-squares (Pattern Matching Analysis) fit obtained, assuming the Pbnm Space Group. Vertical bars below the pattern represent the calculated peak position.

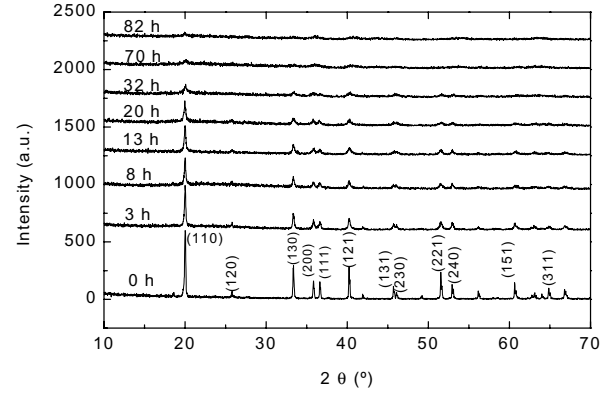

Figure 2 X-Ray diffraction patterns of $Li_2Ti_3O_7$ powders after mechanically grinding for selected times indicated in hours and using an agate container. No extra peaks appear, indicating the absence of decomposition of the powders during the milling process.

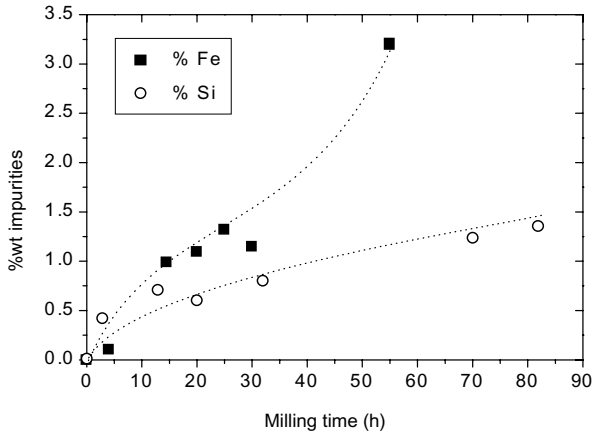

Figure 3 Variation of (a) Si and (b) Fe contamination from both container and balls, with the milling time. Data were determined by EDS analysis.

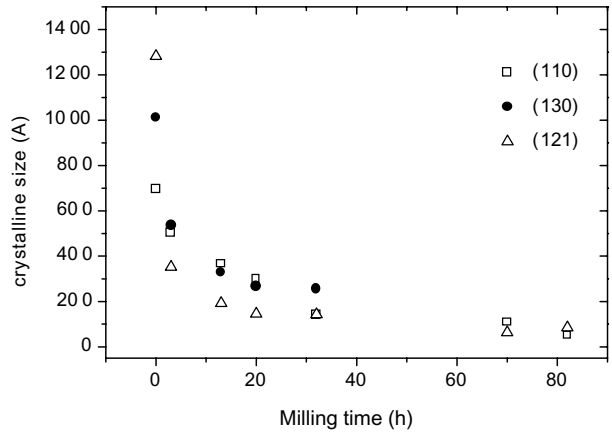

Figure 4 Mean average crystalline size, determined by the Scherrer formula, as a function of milling time.

During the grinding process the powders are in intimate physical contact with the impacting balls as well as with the container chamber walls. This may lead to contamination of the surface that may not be detectable by XRD. Fig. 3 shows the silicon content determined by EDS analysis on the powders obtained after different milling times and using both container and balls made from agate. It can be seen that this silicon content is negligible, if we take into account the detection limit of this technique, however it seems that progressively increases with the milling time. On the other hand, considering that contamination process affects mainly to crystals surface, and EDS is a superficial technique, the amount of Si is clearly being over-estimated. Since no displacement of the diffraction peaks has been observed, the incorporation of silicon atoms to the structure has been discarded.

In order to check if the processed materials can be prepared in an industrial scale, we have performed the milling in a cheap and suitable vessel, as it is an austenite stainless steels (ASS) container. The XRD study made on prepared samples showed that the evolution is similar to that found when agate container was used. However, the contamination problem, in this case with Fe, is slightly higher (see Fig. 3) probably due to difference of hardness and wear behavior between both containers. For this reason we have performed the electrochemical study on the samples prepared in the agate vessel and the results showed here in correspond to the samples processed in this sort of container.

Major sources for line broadening observed in MG specimens are believed to be (1) small coherent domains (crystalline size) and (2) distortion within the coherent domains (microstrain). The size of the coherent domains, also called crystallites, can be estimated from the well known Scherrer equation [20]. In Fig. 4 the apparent crystalline size, L, *versus* milling time deduced from the Scherrer formula for three characteristic diffraction peaks is shown. For all of them the same trend is observed: a decreasing of L with the milling time. However, small difference can be observed especially for unmilled powder where crystalline size varies from 70 to 130 nm depending of the diffraction peaks used. As we have mention before in the experimental part, the crystalline size determined by this method is under-evaluated due to the Scherrer formula does not include the internal strain contribution to peak broadening. In this sense, separation of size and strain components of line broadening can be accomplished using the Hall-Williamson plot [13]: average crystallite size from the intercept on the β axis at $\theta = 0$ and internal strain from the slope of the $\beta \cos\theta - \sin\theta$ plot. Fig. 5 shows an example of these plots for MG powder during 0, 3 and 20 hours. The intercept of the fitted line with the y-axis corresponds to $\beta \cos\theta \approx 0.00099$, 0.00143 and 0.00499° and confirms a fine particle size of about 140, 97 and 28 nm respectively. No correlation for family of crystallographic planes is found, indicating the lack of anisotropic internal strains usually found in metallic samples [21]. Moreover, the fact of β values do not rapidly increase with θ confirms that internal strain is not so important as metallic samples.

Intensities of the crystalline peaks in the XRD patterns (Fig. 2) quickly decrease with milling time and for values higher than 32 hours only the most intense lines, corresponding to (110) planes, can be resolved sufficiently to collect accurate line width data. Therefore, we could use the Williamson-Hall method only for milling time smaller than 32 hours. It can be seen that the results are slightly higher than in the Scherrer calculation mainly due to the fact that internal strain contribution is not considered in the calculation.

Finally we have determined the crystalline size and internal strain with a multiple line profile software, Maud Program (Fig. 6). For grinding times less than 20 hours, crystalline size decreases rapidly to a nanometer scale, while the atomic level strain increases with grinding time. This behavior is explained as formation of defects such as dislocations and/or stacking faults during the process [22, 23]. For grinding times higher than 20 hours the crystalline size also decrease, but at lower rates. This could be interpreted as dislocation movement process is more impeded due to the bonding nature. This behavior departs from that observed for metallic powders where after low milling times a constant value of crystalline size is reached. This fact is explained as a competition of work hardening and recovery process [22–24]. In these terms is explained

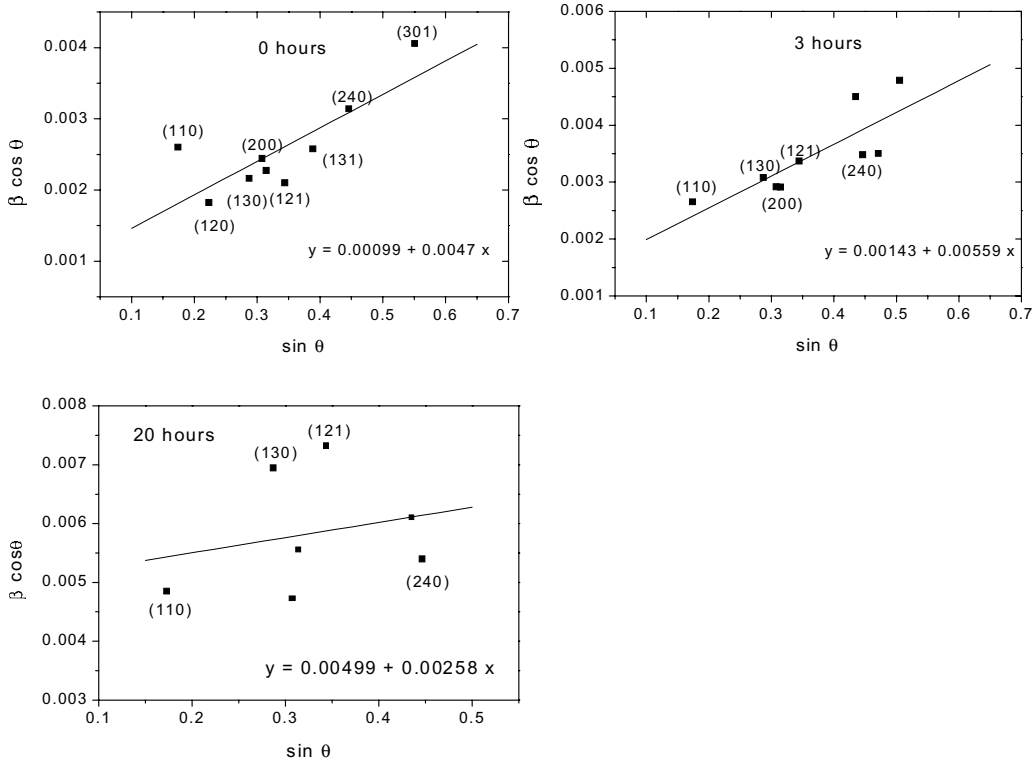

Figure 5 Hall-Williamsom plot showing X-Ray peaks broadening (β) as a function of the Bragg angle (θ) for starting powders and powder milled during 3 and 20 hours.

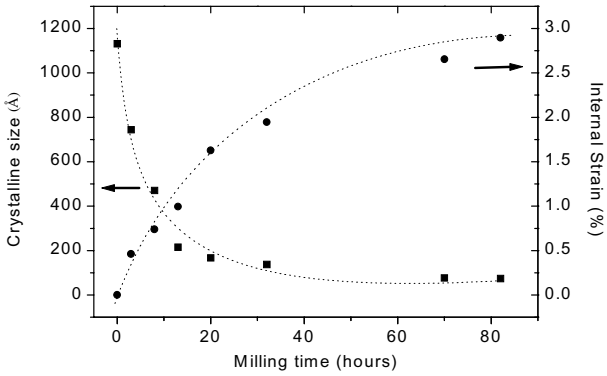

Figure 6 Evolution of crystalline size and internal strain with the milling time obtained from Maud Program for samples processed in the agate vessel.

the behavior of internal strain, where the dislocations are not lost in grain boundaries and the microstrain continuously increases.

3.2. Electrochemical study of MG materials

Fig. 7 shows the first discharge and subsequent charge/discharges cycles at a rate of C/40 (1 Li in 40 hours) for cells using crystalline and milled $Li_2Ti_3O_7$ materials as the positive electrode. Several differences can be noted in the voltage-composition curves depending on the milling time. A smoothing of the V-x slope changes is observed for materials with smaller sizes. This is likely related to the progressive amorphization of $Li_2Ti_3O_7$ detected by X-ray diffraction experiments. To better understand this, one could examine the voltage-intensity representations shown in Fig. 8. In this representation, every intensity minima correspond to a reduction process in which some crystallographic positions are filled with lithium ions. When the energy of these crystallographic sites is well defined, the V-I peaks are sharp, whereas the absence of a fine structure in the cyclic voltammogram means that site energies have gradual and broad energy changes [25]. So, in the studied $Li_2Ti_3O_7$ the shape evolution in both kind of representations, I-V and V-x, could be attached to the fact that amorphous materials present a large spread in the energy of sites in contrast with crystalline materials where the vacant sites are well defined structurally and energetically [26, 27].

The effect of MG is also reflected in the cells polarization, i.e., voltage differences between discharge and charge curves. It can be seen in Fig. 7 that polarization of the cells increases with milling time. Since the configuration of the cathodic pellet as well as experimental setting are the same, we should assume that this is due to the milled grade of the active material. So, the grinding process seems to cause a decrease in the electronic conductivity of the electrode, as has been suggested for other milled compounds [9].

From a technological point of view, one of the most interesting features is the amount of inserted lithium during the consecutive discharging cycles of the cells, i.e., the specific capacity delivered by the cell. As it is well known amorphous samples can intercalate more lithium [28, 29] than the corresponding crystalline materials, therefore they can develop higher specific capacities. If so, an improvement in the performance of $Li_2Ti_3O_7$ should be expected with MG. According to this, at a first view of Fig. 7, it seems that more lithium is inserted under the experimental conditions in long

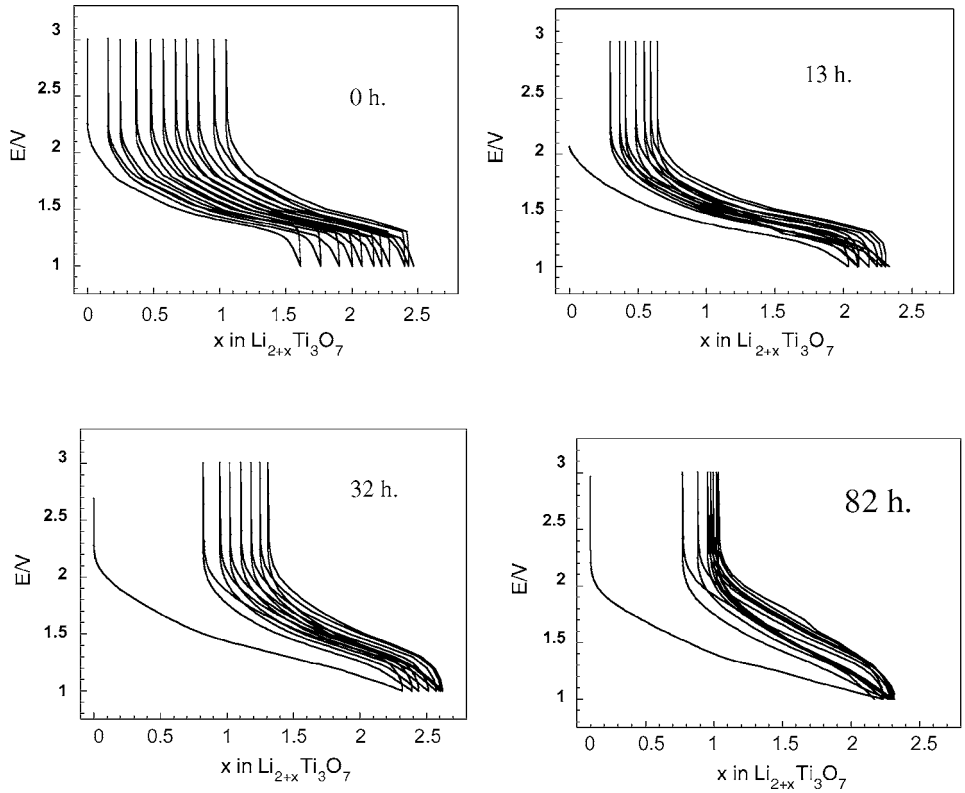

Figure 7 Voltage-composition plot obtained during electrochemical lithium insertion in $Li_2Ti_3O_7$ samples processed through different milling time (0, 13, 32 and 82 hours). The data were collected from cells with the configuration Li/1M $LiPF_6$ in DMC + EC (50 : 50)/$Li_2Ti_3O_7$ cycled at a rate of C/40 (1 Li in 40 hours) between 1 and 3.5 V versus Li^+/Li electrode.

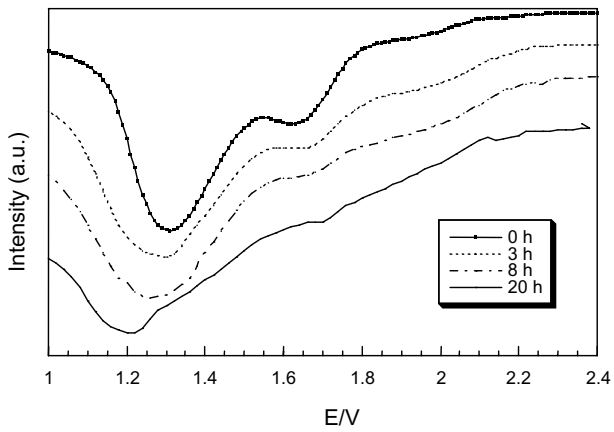

Figure 8 Intensity–voltage curves obtained from a potentiostatic discharge of a Li//$Li_2Ti_3O_7$ cell. Scanning rate was 20 mV/h.

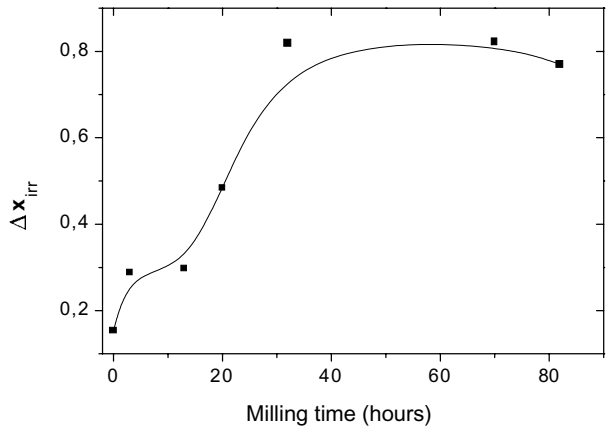

Figure 9 Irreversible capacity as a function of milling time. This irreversible capacity corresponds to the difference of lithium inserted in the first and second discharge of Li//$Li_2Ti_3O_7$ cells.

milled samples, passing from 1.7 during the first cycle in the crystalline material to 2.3 in the sample of $Li_2Ti_3O_7$ grinding for 82 hours. Considering this increase in the specific capacity in the first cycle, mechanical grinding would have a positive effect over the electrochemical properties of materials, being therefore the highly milled compounds the most promising electrode materials.

However mechanical grinding is well known to produce a large amount of defects that could affect the irreversible capacity, Δx_{irr}, [9, 30], which is the difference between inserted Li- deinserted Li in two subsequent discharge-charge cycles of the cell. In Fig. 7, it can be effectively observed that the amount of deinserted lithium ions, Δx_{irr}, is quite different for milled materials in a same cycle number. This can be better observed in Fig. 9 where the irreversible capacity Δx_{irr} is plotted versus the milling time. Actually the irreversible capacity tends to increase with milling time although a minimum is observed at 13 h. Since a high irreversibly capacity supposes a negative characteristic to any electrode material, longest milled compounds are not desirable.

In order to balance the above commented "positive and negative" effect of mechanical grinding in the applicable electrochemical properties, one has to care about the evolution of the reversible specific capacity. Fig. 10 shows the discharging specific capacity with the number of cycles for every cell. It can be seen that in the first cycle the materials ground for long time display the

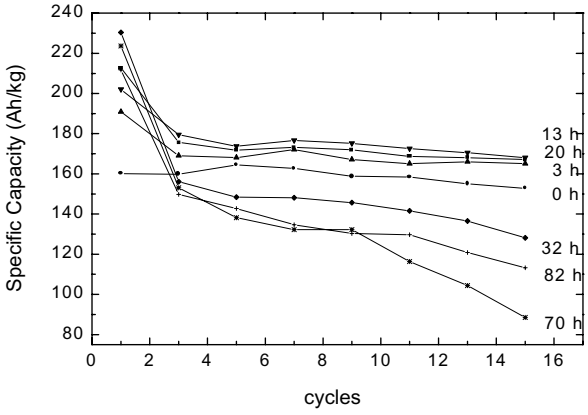

Figure 10 Evolution of the specific capacity developed by milled $Li_2Ti_3O_7$ samples with the number of cycles. Current rate of C/40 (1 Li in 40 hours).

highest capacity, as correspond to its higher amount of intercalated lithium. However, for these compounds, the capacity falls down very fast on cycling. Opposite to this behavior, the compounds milled less than 13 hours presents a more constant value of capacity, and among them the cell bearing the 13 hours milled $Li_2Ti_3O_7$ develops the highest value. This behavior can be understood on the basis of a competition between crystalline size and the internal strain. In general the small grain size improve the diffusion and other superficial process, in particular metallic nanostructured materials, such as Pd [31] or Mg_2Ni [32], show notable hydriding properties in relation to crystalline materials. However, the internal strain likely impede diffusion processes due to the diffusion path inside the unit cell could be dramatically modified. In our case, the crystalline size decreases considerably up to 13 hours of milling time, afterwards it remains basically constant. However above this milling time the internal strain increase greatly (from 1% to 3%).

4. Conclusions

Mechanical grinding of crystalline $Li_2Ti_3O_7$ is possible without producing secondary phases, although slight contamination from the grinding media is unavoidable. The milling process progressively produces an amorphization of the crystalline materials due to both a decreasing of the crystalline size and an increasing of the internal strain. The crystallite size, determined by three different methods, quickly reach a nanometric scale favoring the electrochemical properties, however the evolution of internal strain have opposite behavior and seems to yield electrodes with poor electrochemical characteristics. In this way, MG improves the specify capacity during the first discharge of the cell, but it also increases the irreversible capacity. In this scenario, the optimum compromise is achieved for low milling times (13 h under experimental condition, 20 nm crystallite size). These results demonstrate that MG is an adequate and convenient route to enhance the electrochemical applications of $Li_2Ti_3O_7$ as electrode material.

Acknowledgements

We would like to thank CICYT for supporting the project MAT98-1053-C04 and MAT2001-3713-C04.

References

1. M. E. ARROYO Y DE DOMPABLO, E. MORÁN, A. VÁREZ and F. GARCÍA-ALVARADO, *Mater. Res. Bull.* **32**(8) (1997) 993.
2. S. GARNIER, C. BOHNKE, O. BOHNKE and J. L. FOURQUET, *Solid Stat. Ionics* **83** (1996) 323.
3. C. J. CHEN and M. GREENBLATT, *Mater. Res. Bull* **20** (1985) 1374.
4. M. Y. SONG, E. IVANOV, B. DARRIET, M. PEZAT and P. HAGENMULLER, *Int. J. Hydrogen Energy* **10** (1985) 169.
5. P. ZOLLIKER, K. YVON, P. FISHER and J. SCHEFER, *Inorg. Chem.* **24** (1985) 4177.
6. K. AOKI, H. AOYAGI, A. MEMEZAWA and T. MASUMOTO, *J. Alloys and Comp.* **203** (1994) L7.
7. S. ORIMO and H. FUJII, *ibid.* **232** (1996) L16.
8. J.-L. BOBET, S. PECHEV, B. CHEVALIER and B. DARRIET, *ibid.* **267**(1/2) (1998) 136.
9. F. DISMA, L. AYMARD, L. DUPONT and J. M. TARASCON, *J. Electrochem. Soc.* **143** (1996) 3959.
10. R. PALACIN, G. ROUSSE, M. MORCRETTE, L. DUPONT, C. MASQUELIER, Y. CHABRE and J. M. TARASCON, in Proceedings of the 10th International Meeting on Lithium Batteries, Como, Italy, 2000.
11. P. LEBRUN, L. FROYEN and L. DELAY, *Mater. Sci. Eng.* **A 161** (1993) 75.
12. J. RODRÍGUEZ-CARVAJAL, "Fullprof: A Program for Rietveld Refinement and Pattern Matching Analysis" Vers. 0.2 (1998); *Idem.*, Abstracts of the Satellite Meeting on Powder Diffraction of the XV Congress of the IUCr (Tolouse, France, 1990) p. 117.
13. G. K. WILLIAMSOM and W. H. HALL, *Acta Metall.* **1** (1953) 22.
14. L. LUTTEROTTI, Maud Program. V. 1.63, Univer. Trento, 2000.
15. J. M. TARASCON, *J. Electrochem. Soc.* **132** (1985) 2089.
16. C. MOUGET and Y. CHABRE, Multichannel Potentiostatic and galvanostatic System Macpile, licensed by CNRS and UJF grenoble to Bio-Logic Corp., 1 Avenue de l'Europe, F-38640 Claix, 1991.
17. B. MOROSIN and J. C. MIKKELSEN, *Acta Crystallogr.* B **35** (1979) 798.
18. M. E. RABANAL, A. VÁREZ, B. LEVENFELD and J. M. TORRALBA, *J. Alloys and Compounds*, submitted.
19. M. ZDÚJIC, C. JOVALEKIC, L. J. KARANOVIC, M. MITRIC, D. POLETI and D. SKALA, *Mat. Scienc. & Engineer.* A **245** (1998) 109.
20. B. D. CULLITY, in "Elements of X-Ray Diffraction" (Addison-Wesley, Reading, MA, 1978) p. 284.
21. A. BENGHALEM and D. G. MORRIS, *Acta Metall. Mater* **42**(12) (1994) 4071.
22. C. C. KOCH, *Nanostruct. Mater.* **2** (1993) 109.
23. E. HELLSTERN, H. J. FECHT, Z. FU and W. L. JOHNSON, *J. Appl. Phys.* **65** (1989) 305.
24. A. BOSE in "Advances in Particulate Materials" (Butterworth-Heineman, 1995) p. 162.
25. R. TOSSICI, R. MARASSI, M. BERRETTONI, S. STIZZA and G. PISTOIA, *Solid Stat. Ionics* **67** (1993) 77.
26. K. CHENG and M. S. WHITTINGHAM, *ibid.* **1** (1980) 151.
27. O. BOHNKE and G. ROBERT, *ibid.* **6** (1982) 115.
28. C. JULIEN and G. NAZRI in "Solid State Batteries:Materials Design and Optimization" (Kluwer Academic Publisher, Boston, MA, 1994).
29. R. TOSSICI, R. MARASSI, M. BERRETTONI, S. STIZZA and G. PISTOIA, *Solid Stat. Ionics* **57** (1992) 227.
30. T. ZHENG, J. N. REIMERS and J. R. DAHN, *Phys. Rev.* B **51** (1995) 734.
31. T. MÜTSCHELE and R. KIRCHHEIM, *Scr. Metall.* **21** (1987) 1101.
32. S. ORIMO, H. FUJII and K. IKEDA, *Acta Mater.* **45**(1) (1997) 331.

Received 18 April 2001
and accepted 14 May 2002